On the Superposition Modulation for OFDM-based Optical Wireless Communication

On the superposition modulation for OFDM-based optical wireless communication

Conference Paper · December 2015

DOI: 10.1109/GlobalSIP.2015.7418352

CITATIONS
37

READS
158

3 authors:

Mohamed Sufyan Islim
The University of Edinburgh
30 PUBLICATIONS **473** CITATIONS
SEE PROFILE

Dobroslav Tsonev
The University of Edinburgh
42 PUBLICATIONS **2,636** CITATIONS
SEE PROFILE

Harald Haas
The University of Strathclyde
530 PUBLICATIONS **23,677** CITATIONS
SEE PROFILE

On the Superposition Modulation for OFDM-based Optical Wireless Communication

Mohamed Sufyan Islim, Dobroslav Tsonev and Harald Haas

Li-Fi Research and Development Centre, Institute for Digital Communications
University of Edinburgh, King's Buildings, Mayfield Road, Edinburgh, EH9 3JL, UK
Email: {m.islim, d.tsonev, h.haas}@ed.ac.uk

***Abstract*—Inherent unipolar orthogonal frequency division multiplexing (OFDM) schemes have a reduced spectral efficiency (SE) when compared with direct current (DC)-biased optical OFDM (DCO-OFDM). The concept of superposition modulation was proposed as a solution to the SE loss of unipolar orthogonal frequency division multiplexing (U-OFDM) and the power efficiency loss of pulse-amplitude-modulated discrete multitone modulation (PAM-DMT). In this paper, we demonstrate that the superposition modulation can also be applied to asymmetrically clipped optical OFDM, and we refer to it as enhanced asymmetrically clipped optical OFDM (eACO-OFDM). The eACO-OFDM results in a new power and spectrally efficient scheme for intensity modulation and direct detection (IM/DD) systems. The bit error ratio (BER) performance of the proposed scheme is derived and obtained results agree with Monte Carlo simulations. The performance of the superposition OFDM-based modulation schemes is compared and presented for both additive white Gaussian noise (AWGN) and non-flat visible light communication (VLC) channels.**

I. Introduction

The demand for wireless communication capacity is rapidly increasing. Monthly global mobile data traffic will exceed 24.3 exabytes by 2019 [1]. However, the radio frequency (RF) spectrum is a limited resource. The visible light spectrum offers licence-free bandwidth that can meet these increasing capacity demands. Therefore, visible light communication (VLC) is a promising technique that offers significant energy and cost savings, physical-link level security, and high speed communication links.

VLC employs off-the-shelf light emitting diodes (LEDs) and photodiodes (PDs) as channel front-end devices. The communication signals are restricted to intensity modulation and direct detection (IM/DD) signals. Orthogonal frequency division multiplexing (OFDM) is a good candidate for optical wireless communications due to the simplicity of the single-tap equalizer at the receiver [2]. Hermitian symmetry is generally imposed on the OFDM input frame to enforce the OFDM modulator output to be real. The widely deployed direct current (DC)-biased optical OFDM (DCO-OFDM) uses a DC bias to realize a unipolar signal [3]. However, OFDM signals attain a high peak-to-average power ratio (PAPR) which makes it impossible to convert all of the signal samples into unipolar samples. Following [4], the DC bias is defined as k_M multiple of the standard deviation of the time-domain OFDM signal σ_s, where M is the M-ary quadrature amplitude modulation (M-QAM) modulation order. Therefore, the dissipation of electrical power in DCO-OFDM compared with bipolar OFDM can be written as [4]:

$$B_{\mathrm{DC}}^{\mathrm{dB}} = 10\log_{10}(k_M^2 + 1). \tag{1}$$

This power penalty increases as the modulation order, M, increases, in order to ensure an equivalent lower clipping distortion for all the modulation orders. Unipolar OFDM modulation schemes were introduced to provide an energy efficient alternative to DCO-OFDM. Schemes such as: ACO-OFDM [5]; pulse-amplitude-modulated discrete multitone modulation (PAM-DMT) [6]; flipped OFDM [7]; and unipolar orthogonal frequency division multiplexing (U-OFDM) [8] exploit the OFDM input/output frame structure to realize a unipolar output. However, due to the restrictions imposed on their frame structures, the performance of M-QAM DCO-OFDM, should be compared to M^2-QAM {ACO-OFDM; U-OFDM; flipped-OFDM}, and M-PAM PAM-DMT. Therefore, the power efficiency of these schemes become gradually inefficient as the modulation order, M, increases. Enhanced U-OFDM (eU-OFDM) was proposed as an energy efficient solution to the SE loss of U-OFDM [9]. The concept of eU-OFDM is to superimpose multiple streams of U-OFDM waveforms so that the inter-stream-interference is distortion-less. The SE of each additional stream decreases exponentially as the total number of streams increases. Therefore, achieving a SE equivalent to DCO-OFDM would require a large number of streams to be superimposed. However, due to the computational complexity and memory requirements, practical implementation limits the number of superimposed streams to three typically [10]. Alternatively, different configuration arrangements were exploited in GeneRalizEd ENhancEd UnipolaR OFDM (GREENER-OFDM) to close the SE gap between U-OFDM and DCO-OFDM [11]. In [12], enhanced pulse-amplitude-modulated discrete multitone modulation (ePAM-DMT) was proposed as a superposition modulation for PAM-DMT. In this paper enhanced asymmetrically clipped optical OFDM (eACO-OFDM) is proposed as a power efficient solution to the SE loss of ACO-OFDM. It uses superposition modulation to achieve performance gains. The performance of all of the superposition OFDM-based modulation schemes is compared

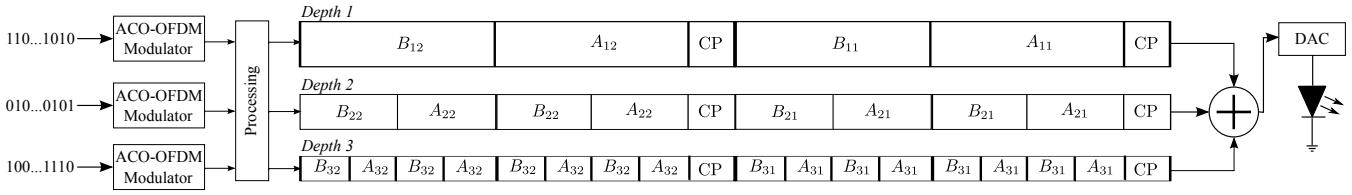

Fig. 1. Illustration of the eACO-OFDM concept with three information streams. CP denotes the cyclic prefix. Subframe A_{dl} represents the first half of unipolar frame, and subframe B_{dl} represents the second half of the unipolar frame. The subscripts denote that the frame at depth-d belongs to the l-th ACO-OFDM frame.

for both the additive white Gaussian noise (AWGN) channel and the non-flat dispersive VLC channel.

A review of ACO-OFDM is given in Section II. The modulation concept and the SE of eACO-OFDM are discussed in Section III. The theoretical analysis is derived in Section IV, and the simulation results and the system comparison are presented in Section V. Conclusions are given in Section VI.

II. ACO-OFDM

The ACO-OFDM scheme exploits the Fourier transformation properties to realize a unipolar signal. If only odd-indexed sub-carriers are loaded with information, the OFDM waveform would have the following property:

$$x[n] = -x[n + N/2], \tag{2}$$

where N is the OFDM frame size. Similarly, if only the even-indexed sub-carriers are used, then the OFDM waveform would have the following property:

$$x[n] = x[n + N/2] \tag{3}$$

A symmetric time domain waveform that follows (2) is achieved in ACO-OFDM [5]. As a result, clipping of the negative values is distortion-less due to the symmetry and all of the distortion will affect the even-indexed sub-carriers. However, skipping half of the sub-carriers results in reducing the SE of ACO-OFDM to half of that in DCO-OFDM. A scaling factor of $\sqrt{2}$ is required to normalize the power as the clipped signal is half of that in the bipolar signal. Therefore, a penalty of 3 dB is applied to the signal-to-noise ratio (SNR) of ACO-OFDM when compared with bipolar OFDM.

III. Enhanced ACO-OFDM

A. Modulation Concept

The symmetry in U-OFDM lies in frames, while in ACO-OFDM and PAM-DMT, it lies in subframes. The main objective of the frame hierarchy design is to convert all of the inter-stream-interference of the superimposed streams into the even-indexed sub-carriers at the frequency domain, so that it becomes distortion-less. A possible arrangement of the multiple ACO-OFDM signals is given in Fig. 1. The eACO-OFDM signal generation starts at the first depth with a conventional ACO-OFDM modulator. The subframes are defined to be half of the original ACO-OFDM frames in length and they are the basic elements of eACO-OFDM streams. At depth-2, a second ACO-OFDM stream is superimposed on the first stream and generated in a similar fashion to depth-1, the OFDM frame length at depth-2 is $N_2 = N_{\mathrm{FFT}}/2$, where N_{FFT} is the OFDM frame length at depth-1. The overall stream at depth-2 is scaled by $1/\sqrt{2}$ in order to preserve the overall signal energy at this depth. Furthermore, ACO-OFDM streams are superimposed at depth-d with an OFDM frame length $N_d = N_{\mathrm{FFT}}/2^{d-1}$ in a similar way as depth-2 and the overall stream at that depth is scaled by $1/\sqrt{2^{d-1}}$. In addition, each of the streams is scaled by a parameter $1/\gamma_d$ to facilitate the optimization of the allocated power to that stream. At the receiver, the demodulation process starts with removing the cyclic prefixes. Then the information carried at depth-1 can be extracted using a traditional ACO-OFDM demodulator. The subframes in each individual frame are symmetric at depth-1. Therefore the information stream at this depth follows (2). At higher depths, the subframes in each individual frame are identical. Therefore the information stream at this depth follows (3). As a result, the odd-indexed sub-carriers only convey the depth-1 information, and the inter-stream-interference falls into the even-indexed sub-carriers. After the information at depth-1 is demodulated, the recovered bits are remodulated at the receiver in order to reconstruct the depth-1 stream, which is then distorted using the channel response and subtracted from the overall eACO-OFDM signal. After the removal of the depth-1 waveform, each two identical subsequent subframes are summed. The demodulation process at depth-2 continues with the conventional ACO-OFDM demodulation process and the recovered bits are remodulated in order to allow for the information stream at depth-2 to be subtracted from the overall received information signal. The demodulation process continues in a similar way for all subsequent streams until the information at the last depth is recovered.

B. Spectral Efficiency

The spectral efficiency of eACO-OFDM is given as the sum of the spectral efficiencies of all ACO-OFDM streams:

$$\eta_{\mathrm{eACO}}(D) = \sum_{d=1}^{D} \eta_{\mathrm{ACO}}(d) \quad \text{bits/s/Hz}, \tag{4}$$

where $\eta_{\mathrm{ACO}}(d)$ is the SE of ACO-OFDM at depth-d:

$$\eta_{\mathrm{ACO}}(d) = \frac{\log_2(M_d)(N_d)}{4(N_1 + N_{\mathrm{CP}})} \quad \text{bits/s/Hz}, \tag{5}$$

where M_d is the constellation size at depth-d. In order for the SE of eACO-OFDM to match that of DCO-OFDM, the

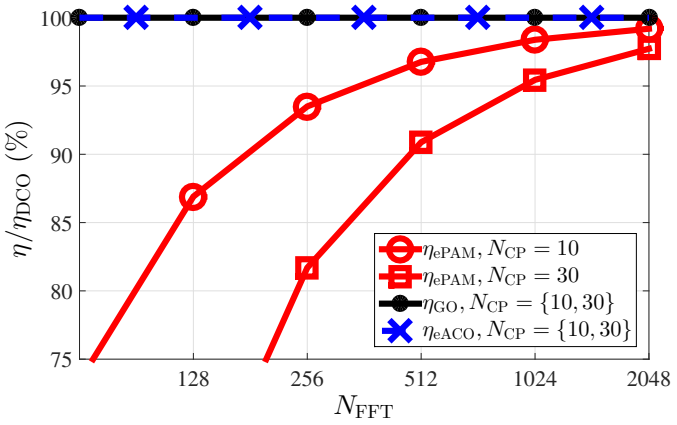

Fig. 2. The spectral efficiency of eACO-OFDM (η_{eACO}), ePAM-DMT (η_{ePAM}), and GREENER-OFDM (η_{GO}) compared to the spectral efficiency of DCO-OFDM (η_{DCO}), as a function of the frame length N and cyclic prefix length $\mathrm{N_{CP}}$.

following criterion should be fulfilled [11]:

$$\log_2(M_{\mathrm{DCO}}) = \sum_{d=1}^{D} \frac{\log_2(M_d)}{2^d}, \tag{6}$$

where M_{DCO} is the constellation size of M_{DCO}-QAM DCO-OFDM. The SE of eACO-OFDM and GREENER-OFDM, η_{GO}, is exactly equivalent to η_{DCO} for any cyclic prefix length. However, The spectral efficiency of ePAM-DMT can never match the spectral efficiency of DCO-OFDM, since multiple cyclic prefixes are employed at higher order depths of ePAM-DMT. This trend is shown in Fig. 2 as a function of the OFDM frame and cyclic prefixes lengths. It is shown that the spectral efficiency of ePAM-DMT, η_{ePAM}, exceeds 90% of η_{DCO} for all of the presented cyclic prefix lengths when the frame size $N \geq 512$.

IV. Theoretical Analysis

The VLC channel model is given by:

$$\mathbf{y} = \mathbf{H}\mathbf{x} + \mathbf{w}, \tag{7}$$

where $\mathbf{x}$ and $\mathbf{y}$ are the transmitted and received superposition-modulated time domain waveforms; $\mathbf{w} = \{w_i; i = 0, 1, ..., N-1\}$ is the AWGN samples, $w_i \sim \mathcal{N}(0, N_o)$, where N_o is the double-sided power spectral density (PSD) of the noise at the receiver; and $\mathbf{H}$ is a $N \times N$ circulant convolution channel matrix with the first column representing the channel impulse response $\mathbf{h} = [h_0, h_1, ..., h_L, 0, ..., 0]^{\mathrm{T}}$, where L is the number of channel taps. The channel matrix $\mathbf{H}$ can be diagonalized as:

$$\mathbf{H} = \mathbf{F}^* \mathbf{\Lambda} \mathbf{F}, \tag{8}$$

where $\mathbf{F}$ is an $N \times N$ discrete Fourier transform (DFT) matrix, and $\mathbf{\Lambda}$ is an $N \times N$ diagonal matrix with the eigenvalues of the channel $\mathbf{\Lambda} = [\Lambda_0, \Lambda_1, ..., \Lambda_N]^{\mathrm{T}}$.

ACO-OFDM, PAM-DMT and U-OFDM waveforms follow a truncated Gaussian distribution. Therefore, the statistics of these schemes are identical. The statistics of their superposition forms are also identical. The power is allocated to each stream so that the average electrical and optical power of the modulation signal satisfy the following constraint:

$$\begin{aligned} P_{\mathrm{elec}}^{\mathrm{avg}}(D, \underline{\gamma}) &\leq P_{\mathrm{elec}}^{\mathrm{avg}}(D, \mathbf{1}_{1\times D}), \\ P_{\mathrm{opt}}^{\mathrm{avg}}(D, \underline{\gamma}) &\leq P_{\mathrm{opt}}^{\mathrm{avg}}(D, \mathbf{1}_{1\times D}), \end{aligned} \tag{9}$$

where $\underline{\gamma} = \{\gamma_d^{-1}; d = 1, 2, \ldots, D\}$ is the set of scaling factors applied to each corresponding stream; $P_{\mathrm{elec}}^{\mathrm{avg}}(D, \underline{\gamma})$ and $P_{\mathrm{opt}}^{\mathrm{avg}}(D, \underline{\gamma})$ are the average electrical and optical power for the superposition-modulated OFDM-based waveform, respectively.

A theoretical bound on the bit error ratio (BER) performance of the superposition-modulated streams can be derived using the formula for the BER performance of real bipolar M-QAM-OFDM [13]. For eACO-OFDM, the achieved electrical SNR at the receiver should be scaled by a factor of $1/2$ to account for the SNR loss in ACO-OFDM, and by $1/\alpha_{\mathrm{elec}}^{\mathrm{eACO}}(D, d)$ to account for the electrical SNR penalty in eACO-OFDM, where $\alpha_{\mathrm{elec}}^{\mathrm{eACO}}(D, d)$ denotes the increase in the dissipated electrical energy per bit in eACO-OFDM compared with the electrical energy dissipation per bit in ACO-OFDM stream at depth-d [11]. A multipath dispersive VLC channel is adopted [14, Fig. 3] and a zero-forcing equalizer is used for simplicity as the objective is to prove the validity of superposition OFDM-based schemes in non-flat channels. The BER performance at depth-d can be expressed as:

$$\begin{aligned} \mathrm{BER}_{(D,d,\underline{\gamma})}^{\mathrm{eACO}} \cong \frac{4}{\log_2(M_d)} \left(1 - \frac{1}{\sqrt{M_d}}\right) \times \\ \sum_{l=1}^{R} \sum_{k=1}^{N} \mathrm{Q}\left((2l-1)\sqrt{\frac{3|\Lambda_k|^2 E_{\mathrm{b,elec}} \log_2(M_d)}{2\alpha_{\mathrm{elec}}^{\mathrm{eACO}}(D, d)(M_d - 1)N_{\mathrm{o}}}}\right), \end{aligned} \tag{10}$$

where $E_{\mathrm{b,elec}}/N_{\mathrm{o}}$ is the SNR of real bipolar OFDM, and $R = \min(2, \sqrt{M_d})$. For flat channels, $\mathbf{\Lambda} = I_N$.

The BER performance at higher depths is affected by the BER performance of the streams at the lower depths. Any incorrectly decoded bit at lower order depths translates into more distortion for all subsequent streams. The presented solution does not include the effects of the error propagation due to errors in preceding streams which results in an underestimation of the BER at low SNR values. However, for high SNR values, this error propagation effect is assumed to be insignificant due to the low BER expected at each stream. A closed-form bound on the average BER performance of the overall eACO-OFDM scheme can be obtained by considering the spectral contribution of each individual stream to the overall BER. The average BER performance can then be expressed as:

$$\mathrm{BER}^{\mathrm{eACO}} \cong \sum_{d=1}^{D} \left(\mathrm{BER}_{(D,d,\underline{\gamma})}^{\mathrm{eACO}} \xi_d\right), \tag{11}$$

where ξ_d is the effective spectral contribution of the stream at depth-d to the overall SE. The BER performance bound as a function of the optical SNR can be obtained by inserting

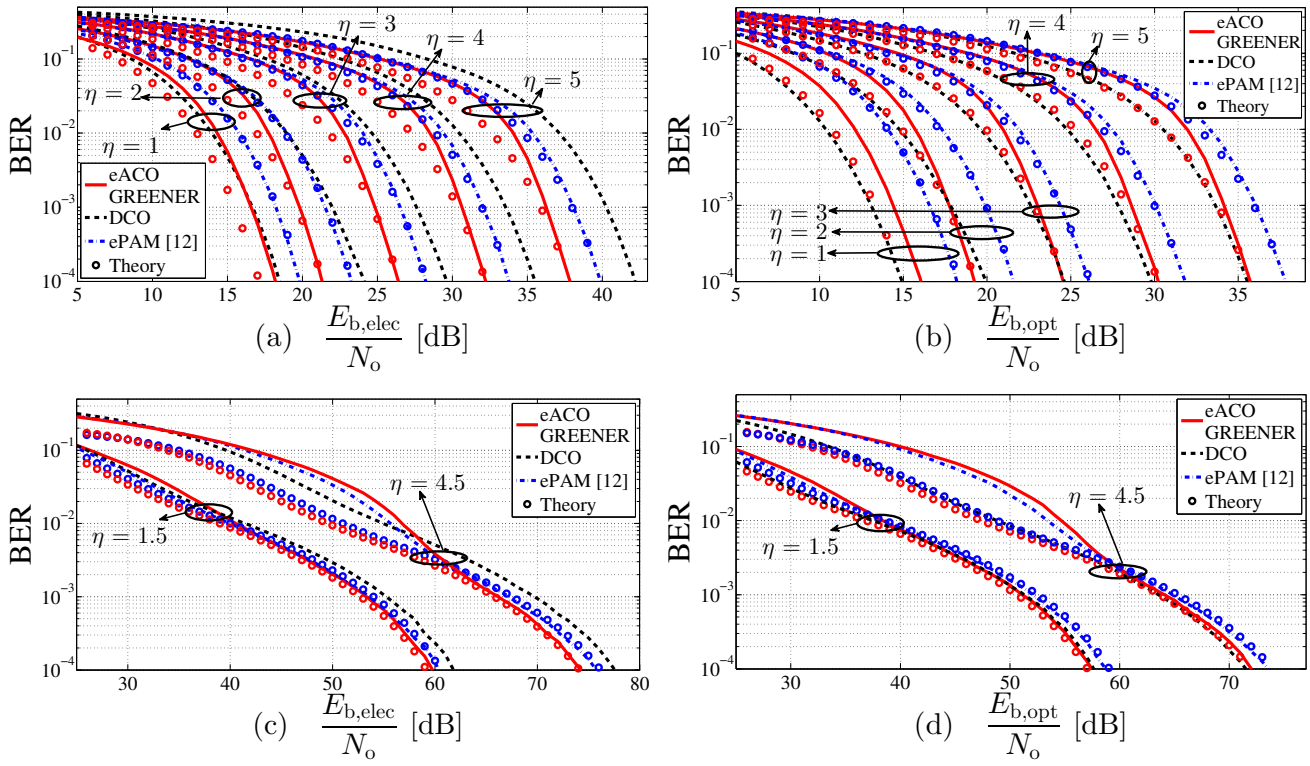

Fig. 3. The BER performance of eACO-OFDM versus ePAM-DMT versus GREENER-OFDM versus DCO-OFDM for different spectral efficiencies, in both AWGN channel (a and b) and dispersive channel (c d), as a function of electrical SNR, and optical SNR. The value of η is given in bits/s/Hz. DC bias levels for DCO-OFDM at $\eta = \{1, 1.5, 2, 3, 4, 4.5, 5\}$ are estimated through Monte Carlo simulations at respectively 6, 7, 7.5, 9.5, 11, 12, and 13 dB as described in (1).

the ratio of average optical power to the the average electrical power, defined in [11], into (10).

V. Simulation Results

The optimal configurations (optimal combinations of constellation sizes and their corresponding scaling factors) for eACO-OFDM are identical to GREENER-OFDM due to the similarity in signal statistics and system design; and the optimal configurations for ePAM-DMT are different due to the different system design [12]. The performance of the optimum configurations in all superposition modulation schemes is compared with the performance of a spectrally equivalent DCO-OFDM in both the AWGN channel and the dispersive VLC channel. The only non-linear effect considered is the negative clipping of the modulation signal due to the characteristics of an ideal LED. The DCO-OFDM DC bias levels for the different M-QAM DCO-OFDM are estimated using Monte Carlo simulations [15]. The performance results are presented for BER values down to 10^{-4} since most of the forward error correction (FEC) codes would be able to maintain a reliable communication link at such BER values [16]. The BER performance of the superposition OFDM schemes in an AWGN channel is presented in Fig. 3(a and b), and equivalent trends are shown in Fig. 3(c and d) for the non-flat dispersive VLC channel [14]. The SE for all of the presented schemes is higher than 97% of the SE of DCO-OFDM. The eACO-OFDM/GREENER-OFDM performances are equivalent for all cases, since the optimal configurations used are identical. The electrical energy savings for eACO-OFDM/GREENER-OFDM start at 1 bit/s/Hz, while for ePAM-DMT [12, eq. (15)], the electrical energy savings start at 1.5 bits/s/Hz. As shown in Fig. 3(a and c), the superposition OFDM-based schemes are more efficient in terms of the electrical SNR requirements when compared with DCO-OFDM, with an advantage for eACO-OFDM/GREENER-OFDM over ePAM-DMT. For the optical SNR values, the eACO-OFDM/GREENER-OFDM schemes are shown to have an equivalent performance to DCO-OFDM for most of the presented cases, however, the performance of DCO-OFDM is more efficient when compared with the ePAM-DMT, as shown Fig. 3(b and d). At high SNR values, the theoretical BER values are in close agreement with Monte Carlo results for all the presented cases.

VI. Conclusion

The superposition modulation concept is extended to ACO-OFDM. The spectral efficiency (SE) of the proposed scheme, eACO-OFDM, is equivalent to DCO-OFDM. A theoretical bound on the BER performance of eACO-OFDM is derived and agrees with Monte Carlo simulations. The performance of all superposition OFDM-based schemes is compared with DCO-OFDM in both AWGN and in multipath dispersive channels. The BER performance of eACO-OFDM and GREENER-OFDM are equivalent. Future research will consider the LED non-linearity and PAPR.

REFERENCES

[1] Cisco Visual Networking Index, "Global Mobile Data Traffic Forecast Update, 2014-2019," CISCO, White Paper, Feb. 2015. [Online]. Available: http://www.cisco.com/c/en/us/solutions/collateral/service-provider/visual-networking-index-vni/white_paper_c11-520862.pdf

[2] S. Dimitrov and H. Haas, *Principles of LED Light Communications: Towards Networked Li-Fi*. Cambridge University Press, 2015.

[3] J. B. Carruthers and J. M. Kahn, "Multiple-subcarrier Modulation for Nondirected Wireless Infrared Communication," *IEEE Journal on Selected Areas in Communications*, vol. 14, no. 3, pp. 538–546, Apr. 1996.

[4] J. Armstrong and B. J. C. Schmidt, "Comparison of Asymmetrically Clipped Optical OFDM and DC-Biased Optical OFDM in AWGN," *IEEE Commun. Lett.*, vol. 12, no. 5, pp. 343–345, May 2008.

[5] J. Armstrong and A. Lowery, "Power Efficient Optical OFDM," *Electronics Letters*, vol. 42, no. 6, pp. 370–372, Mar. 16, 2006.

[6] S. C. J. Lee, S. Randel, F. Breyer, and A. M. J. Koonen, "PAM-DMT for Intensity-Modulated and Direct-Detection Optical Communication Systems," *IEEE Photonics Technology Letters*, vol. 21, no. 23, pp. 1749–1751, Dec. 2009.

[7] N. Fernando, Y. Hong, and E. Viterbo, "Flip-OFDM for Unipolar Communication Systems," *IEEE Transactions on Communications*, vol. 60, no. 12, pp. 3726–3733, Dec. 2012.

[8] D. Tsonev, S. Sinanović, and H. Haas, "Novel Unipolar Orthogonal Frequency Division Multiplexing (U-OFDM) for Optical Wireless," in *Proc. of the Vehicular Technology Conference (VTC Spring)*, IEEE. Yokohama, Japan: IEEE, May 6–9 2012.

[9] D. Tsonev and H. Haas, "Avoiding Spectral Efficiency Loss in Unipolar OFDM for Optical Wireless Communication," in *Proc. of the International Conference on Communications (ICC)*. Sydney, Australia: IEEE, Jun., 10–14 2014.

[10] D. Tsonev, S. Videv, and H. Haas, "Unlocking Spectral Efficiency in Intensity Modulation and Direct Detection Systems," *IEEE J. Sel. Areas Commun.*, vol. PP, no. 99, pp. 1–1, 2015.

[11] M. Islim, D. Tsonev, and H. Haas, "A Generalized Solution to the Spectral Efficiency Loss in Unipolar Optical OFDM-based Systems," in *Proc. of the International Conference on Communications (ICC)*. London, UK: IEEE, Jun., 8–12 2015.

[12] ——, "Spectrally Enhanced PAM-DMT for IM/DD Optical Wireless Communications," in *Proc. of the 25th Int. Symp. Pers. Indoor and Mobile Radio Commun. (PIMRC)*. Hong Kong, China: IEEE, Aug. 30–Sep. 2 2015, pp. 927–932.

[13] F. Xiong, *Digital Modulation Techniques*, 2nd ed. Artech House Publishers, 2006.

[14] K. Lee, H. Park, and J. Barry, "Indoor channel characteristics for visible light communications," *IEEE Communications Letters*, vol. 15, no. 2, pp. 217 – 219, Feb. 2011.

[15] S. Dimitrov, S. Sinanovic, and H. Haas, "Clipping Noise in OFDM-Based Optical Wireless Communication Systems," *IEEE Transactions on Communications*, vol. 60, no. 4, pp. 1072–1081, April 2012.

[16] ITU-T, "Forward error correction for high bit-rate DWDM submarine systems," ITU, Tech. Rep. ITU-T G.975.1, Retrieved Nov. 19, 2013 from http://www.itu.int/rec/T-REC-G.975.1-200402-I/en, 2004.